

Kepler and the seven dwarfs: detection of low-level day-timescale periodic photometric variations in white dwarfs

Dan Maoz, Tsevi Mazeh, Amy McQuillan

School of Physics and Astronomy, Tel-Aviv University, Tel-Aviv 69978, Israel

9 December 2014

ABSTRACT

We make use of the high photometric precision of *Kepler* to search for periodic modulations among 14 normal (DA- and DB-type, likely non-magnetic) hot white dwarfs (WDs). In five, and possibly up to seven of the WDs, we detect periodic, ~ 2 hr to 10 d, variations, with semi-amplitudes of 60–2000 ppm, lower than ever seen in WDs. We consider various explanations: WD rotation combined with magnetic cool spots; rotation combined with magnetic dichroism; rotation combined with hot spots from an interstellar-medium accretion flow; transits by size ~ 50 –200 km objects; relativistic beaming due to reflex motion caused by a cool companion WD; or reflection/re-radiation of the primary WD light by a brown-dwarf or giant-planet companion, undergoing illumination phases as it orbits the WD. Each mechanism could be behind some of the variable WDs, but could not be responsible for all five to seven variable cases. Alternatively, the periodicity may arise from UV metal-line opacity, associated with accretion of rocky material, a phenomenon seen in $\sim 50\%$ of hot WDs. Non-uniform UV opacity, combined with WD rotation and fluorescent optical re-emission of the absorbed UV energy, could perhaps explain our findings. Even if reflection by a planet is the cause in only a few of the seven cases, it would imply that hot Jupiters are very common around WDs. If some of the rotation-related mechanisms are at work, then normal WDs rotate as slowly as do peculiar WDs, the only kind for which precise rotation measurements have been possible to date.

Key words: stars: white dwarfs

1 INTRODUCTION

The final stage of stellar evolution, in which an intermediate-mass star loses a significant fraction of its mass and becomes a white dwarf (WD), is still incompletely understood theoretically, and poorly constrained observationally. Photometric variability can inform the problem by revealing WD rotation and WD companions — planetary, substellar, or stellar remnants.

For normal stars, the high photometric precision of the *Kepler* mission has revolutionised our knowledge of both companions and rotation. By detecting planetary transits, *Kepler* has discovered over 3500 planet candidates (Batalha et al. 2013), and more than 2000 eclipsing binaries (Slawson et al. 2011). The BEER project (Faigler & Mazeh 2011) is finding tens of companions to *Kepler* stars through photometric modulation due to combinations of relativistic beaming, tidally induced ellipticity, and reflection of the companion’s light (Faigler et al. 2012). Rotation periods have been measured for 34,000 main-sequence

stars, based on star-spot-induced photometric modulation (McQuillan et al. 2014).

In this paper, we attempt to apply *Kepler*’s unique capabilities to probe for rotation and companions in WDs. We briefly review the observational state of the art regarding each of these phenomena.

1.1 WD rotation

The rotation speed of a WD is one of the few remnant clues to the physics of WD formation. If angular momentum were conserved during the formation of a degenerate stellar core, one would expect a factor of $\sim 10^4$ spinup. For the typical ~ 10 day periods of main-sequence stars (McQuillan et al. 2014), minute-scale rotation periods would be expected. However, as summarised below, typical observed WD rotation periods are of order 1 day. Recent astroseismology of 300 red giants using *Kepler* indicates that the degenerate stellar cores are slowly rotating already at the last stages of the red giant branch (Mosser et al. 2012), slower than currently ex-

plainable by stellar evolution models (Cantiello et al. 2014). An additional, later, source or sink of angular momentum for WDs in close binaries could be torques induced during common-envelope phases, Roche-lobe overflow accretion from a companion, or merger with another WD or stellar core (e.g. Tout et al. 2008).

The theoretical possibility of fast WD rotation has been raised recently within the “spinup/spindown” scenario (Yoon & Langer 2004; Di Stefano et al. 2011; Justham 2011; Ilkov & Soker 2012) of Type-Ia supernovae (SNe Ia), in which an accreting WD could gain enough angular momentum to be rotationally supported against contraction and ignition as a SN Ia, beyond the Chandrasekhar limit. This would also be a way of explaining some “super-Chandrasekhar-mass” SNe Ia, in which the luminosity of the events suggests an exploding mass significantly above the Chandrasekhar mass (e.g. Howell et al. 2006; Silverman et al. 2011; Kamiya et al. 2012). However, to attain rotational support at masses significantly above the non-rotating limit, WDs must have differential rotation, but instabilities and magnetic torqueing might prevent this. A handful of WDs for which rotation profiles have been derived via asteroseismology are indeed consistent with solid-body rotation (Fontaine et al. 2013). If spinup/spindown were a dominant SN Ia channel, the Galactic SN Ia rate per unit stellar mass, the local stellar mass density, and local density of WDs, together imply that $\sim 10^{-4} - 10^{-2}$ of the WD population would be fast rotators, with periods of order 20 s (i.e. near breakup speed), for spindown times of 0.1-10 Gyr, respectively (Maoz et al. 2014). More generally, the existence or absence of WDs even with moderately fast spin periods, of order minutes, could inform the question of whether sustained fast WD rotation is at all possible.

Observationally, measurement of WD rotation is difficult. The absorption lines of hydrogen and helium in the spectra of the most common DA- and DB-type WDs, respectively, are highly pressure-broadened, but have a weak narrower NLTE line core that is observable in H α and H β . Spectroscopic estimates of rotational broadening of the NLTE core are quite uncertain, or give only upper limits (see e.g. Karl et al. 2005, who obtain projected rotational velocity estimates for about 20 DA WDs). As detailed below, more precise WD rotation measurements have been mostly limited to relatively rare types of WDs — magnetic WDs, by means of photometric variability, and WDs with optical-range metal lines, based on spectroscopic observation of their rotation-broadened NLTE metal-line cores.

Some 10-20% of WDs have surface magnetic fields $B \gtrsim 10$ kG, and about 5% have $B \gtrsim 1$ MG (Kawka et al. 2007; Holberg et al. 2008; Kepler et al. 2013). Magnetic fields can be estimated from Zeeman-splitting of absorption-line cores, or by spectropolarimetric measurements of circular polarization variations across line profiles. For strong magnetic fields, variations in the parallel component of the surface field can lead to “magnetic dichroism” — a net circular polarization due to a dependence of continuum opacity on field strength. The net circular polarization, expressed by the ratio of Stokes parameters, depends on magnetic field roughly as $V/I \sim B/(10^9 \text{ G})$ (Angel et al. 1981). Thus, when $B \gtrsim 100$ MG, this effect can lead, in rotating WDs, to periodic photometric variations of order 10%, (e.g. Ferrario et al. 1997).

In the less strongly magnetic WDs, localized star spots may be able to form at sites where the magnetic field inhibits convective motions, resulting in lower effective temperatures there. Combined with rotation, this can possibly lead to photometric modulation. Because the atmospheres of DA-type WDs are expected to become fully radiative above $T_{\text{eff}} = 12,000\text{--}14,000$ K, and DB WDs above $T_{\text{eff}} = 23,000\text{--}28,000$ K, hot WDs are not expected to have spots (Brinkworth et al. 2005). Brinkworth et al. (2013) have searched for photometric variability among 23 magnetic WDs. Including some previously known results, they obtain periods for 10 WDs, and rough possible period ranges for another 7, with typical amplitudes of 1–2%. They interpret these results as rotation periods made observable by cool magnetic spots.

A second class of WDs permitting detection of rotation are DAZ- DBZ- and DZ-type, i.e. WDs displaying, in addition to hydrogen or helium in their atmospheres, strong metal lines in their optical spectra (produced by pollution of the photospheres by accreted dust or rocky material; Farihi et al. 2013). Metal-rich WDs constitute $\sim 10\text{--}20\%$ of all WDs (Holberg et al. 2008). Because of their higher atomic weight, the NLTE line cores of the metal lines have smaller intrinsic thermal widths than those of the hydrogen lines, facilitating the measurement of rotational broadening. Among 38 DAZ WDs, Berger et al. (2005) measured projected rotation speeds for 10 WDs, and upper limits of $v \sin i < 10 \text{ km s}^{-1}$ for the other 28 objects.

Finally, WD rotation can be measured by means of asteroseismology of WDs that have cooled, after a few 100 Myr, to effective temperatures of $T_{\text{eff}} \sim 12,000$ K, at which point they undergo non-radial g -mode pulsations. The pulsations typically have periods of $\sim 100\text{--}1000$ s, and up to ~ 1 hr in very low-mass WDs (Winget & Kepler 2008). WD rotation can induce splitting of pulsation frequencies in the power spectrum. Kawaler (2004) summarizes rotation periods obtained for 10 pulsating WDs in this way. A recent measurement of this type by Greiss et al. (2014) using the *Kepler* Mission, for the DA WD KIC 11911480, reveals a rotation period of 3.5 d.

Based on the various methods, the successful detections of rotation, for ≈ 50 WDs in total, indicate slow rotations. WD period distributions center on periods of order a day, with few periods of less than ~ 30 min [e.g. Kawaler 2004; see Ferrario et al. 1997, for an isolated (i.e. not in an interacting binary) hot WD, likely a merger remnant, with a 12 min period], but with many lower limits suggesting significantly longer periods. However, this is a small number of WDs, and the studied stars are not from among the most common WD types — they are either magnetic, with metal-rich atmospheres, or in the narrow temperature range in which pulsations occur. Rotation periods for larger samples of normal WDs would reveal the distribution of angular momentum for the WD population as a whole.

1.2 Close companions to WDs

Substellar and stellar-remnant companions to WDs can not only provide clues to the final stages of stellar evolution, but may well play an important role in that evolution, e.g. by stripping stellar envelopes during common-envelope phases (e.g. Soker 2013). Brown-dwarf + WD systems permit age-

dating the brown dwarfs, and are important for understanding their physics and demography (e.g. Debes et al. 2011). Close double-WD systems are tracers of stellar multiplicity (e.g. Badenes & Maoz 2012), prime candidates for SN Ia progenitors (e.g. Maoz et al. 2014), and the main sources for future space-based gravitational wave experiments (e.g. Amaro-Seoane et al. 2013). Planets in the habitable zones of WDs (Agol 2011) may hold the best hopes for the detection of biomarkers (Loeb & Maoz 2013). The statistics of these populations have begun to emerge, but much is yet to be learned.

A handful of brown-dwarf companions to WDs is known (see, e.g. summary in Debes et al. 2011), but it is clear that such systems are rare, in analogy to the “brown-dwarf desert” of main-sequence stars. Based on near-infrared excesses in samples of WDs from SDSS, Steele et al. (2011) and Girven et al. (2011) have estimated that ~ 0.5 to 2 per cent of WDs have brown-dwarf companions.

About 50 close double WD systems are known, and statistical studies have estimated the fraction of such systems among WDs at 2 to 20% (Maxted & Marsh 1999). More recently, Badenes & Maoz (2012) found, among 4000 WD spectra from SDSS, 15 WDs with observed RV changes of $> 250 \text{ km s}^{-1}$ between consecutive (~ 15 min) exposures, strongly suggestive of double-WDs with separations $a < 0.05 \text{ AU}$, corresponding to periods of up to about 4 days, for typical WD masses. A statistical analysis interprets this result into a ~ 5 –10% true fraction of such systems among WDs.

Turning to planets around WDs, there are no *bona fide* known cases of WDs with planets, but there is growing circumstantial evidence for their possible existence, despite theoretical questions if planets can survive engulfment by their parent stars during the giant stages (e.g. Villaver & Livio 2009; Nordhaus & Spiegel 2013). For example, Charpinet et al. (2011) have used *Kepler* to deduce the presence of two Earth-sized planets orbiting a hot B subdwarf star (a red giant stripped of its envelope, and destined to become a WD), with 5.7 hr and 8.2 hr periods. Reflection or thermal re-emission of the WD radiation by the planets modulates the WD light by ~ 50 ppm. Circumstellar disks of gas and dust are seen in some WDs, by means of mid-infrared excesses (e.g. Hoard et al. 2013). Koester et al. (2014) used Hubble Space Telescope ultraviolet spectroscopy of 85 DA WDs to identify accreted refractory elements in their atmospheres, and deduce that 27% to 50% of the WDs are currently accreting planetary debris. This material is predominantly of a rocky nature, occasionally even differentiated (Gänsicke et al. 2012). In one WD, Farihi et al. (2013) conclude from analysing the abundance of oxygen in the WD atmosphere that the accreted material consisted of 26% water, presumably from an asteroid-sized object that was tidally disrupted and accreted. Debes et al. (2012) argue that the accreted planetesimals are perturbed into their close orbits via resonance with a Jupiter-mass planet. In summary, the discovery of planets around WDs may be around the corner.

1.3 *Kepler* in quest of companions and rotation in a small sample of WDs

Below, we search for possible signs of companions and rotation in a sample of 14 normal WDs observed by *Kepler*. We detect and measure periodicity in at least five, and possibly up to seven of the 14 WDs, based on photometric variations much smaller than those detectable by previous WD variability studies. We then discuss the possible physical origins of the observed modulations.

2 SAMPLE SELECTION

A sample of 14 WDs was observed with *Kepler* and studied by Østensen et al. (2010, 2011), as part of a program to search for pulsations among compact stars (with a null result for pulsations among the WDs in the sample). The sample is listed in table 3 of Østensen et al. (2011), which is partly reproduced here in Table 1, including the WD types, effective temperatures (T_{eff} , to accuracies of $\pm 500 \text{ K}$), and surface gravities ($\log g$, to accuracies of ± 0.3), as derived spectroscopically by Østensen et al. (2011). The gravities and temperatures, combined with models for WD radius vs. mass and temperature (e.g. Wood 1995) permit estimating the WD mass to $\sim \pm 0.2 M_{\odot}$.

Among these 14 WDs, one (WD1942+499 = KIC 11822535, a $T_{\text{eff}} = 36,000 \text{ K}$ DA WD) was a previously known WD in the *Kepler* field; eight WDs were discovered among candidates selected based on UV-excess in *Galex* photometry (Martin et al. 2005); two were selected based on UV excess in the SDSS-SEGUE survey (Yanny et al. 2009); and seven WDs were chosen from the USNO catalog based on the method of reduced proper motions, which detects relatively faint objects with large proper motions, i.e. nearby low-luminosity stars, primarily WDs. Several of the 14 WDs were found by more than one of these selection methods, and all 14 were spectroscopically confirmed as WDs and classified by Østensen et al. (2010, 2011).

Significantly for our objective of possibly measuring rotation in normal WDs, there is no selection effect in the sample that would obviously favour magnetic WDs. The fraction of magnetic WDs among the 14 is thus likely similar to the magnetic fraction in the WD population as a whole, i.e. one or two WDs may be magnetic. The sample selection methods do result, however, in a hot WD sample, with all but one having $T_{\text{eff}} > 14,000 \text{ K}$, implying cooling ages of order 10^8 yr or less. Twelve WDs are DA-type, one is a DB-type, and one target (KIC 7129927) is likely a double-degenerate system of two DA WDs of comparable brightness, based the spectral fitting of the Balmer-line profiles Østensen et al. (2011).

Apart from the “long cadence” (~ 30 min) data available for all *Kepler* targets, these 14 WDs also have “short cadence” (~ 1 min) data, which permits searching for short periods. Our analysis makes use of Public Releases 14–21 of the long cadence data, and Public Release 21 of the short cadence data, which were downloaded from the *Kepler* mission archive¹. Table 1 includes the quarters of data available for each WD, ranging from Q1–Q17. Only a fraction of this

¹ <http://archive.stsci.edu/kepler>

Table 1. White dwarfs

KIC	RA [deg]	Dec [deg]	Kp [mag]	T_{eff} [kK]	$\log g$ [cm/s ²]	Type	Qtrs LC	Qtrs SC	Period [days]	A [ppm]
Periodic										
5769827	283.688	41.088	16.6	66	8.2	DA	4,6	4	8.30 ± 0.04	818 ± 44
6669882	283.942	42.118	17.9	30.5	7.4	DA	2	2	0.367 ± 0.009	821 ± 16
6862653	291.692	42.327	18.2	16	–	DB	2	2	0.594 ± 0.02	507 ± 21
8682822	289.336	44.878	15.8	23.1	8.5	DA	5-9	1,5	4.7 ± 0.3	60 ± 10
11337598	284.446	49.161	16.1	22.8	8.6	DA	3,10	3	0.09328 ± 0.00003	311 ± 30
11514682	295.302	49.419	15.7	32.2	7.5	DA	3-14	2	9.89 ± 0.06	62 ± 6
11604781	288.537	49.611	16.7	9.1	8.3	DA	3,6,7	3	4.89 ± 0.02	2060 ± 30
Non-periodic										
3427482	286.344	38.526	17.3	–	–	DA	1	1	–	< 600
4829241	289.865	39.978	15.8	19.4	7.8	DA	3-9	1,5	–	< 50
7129927	295.247	42.675	16.6	–	–	DA+DA3,5,6	3	3	–	< 80
9139775	284.432	45.539	17.9	24.6	8.6	DA	2	2	–	< 700
10198116	287.497	47.286	16.4	14.2	7.9	DA	4-6	4	–	< 70
10420021	297.311	47.579	16.2	16.2	7.8	DA	5-10	2,5,6	–	< 50
11822535	295.932	50.077	14.8	36.0	7.9	DA	3-9	2,5-13	–	< 20

time span was available to Østensen et al. (2010, 2011) at the time of their study of this sample.

3 TIME SERIES ANALYSIS

3.1 Method

To search for periodic or quasiperiodic photometric modulation in the WD light curves, we calculated for each WD a fast Fourier transform (FFT) with zero padding, and visually examined the power spectra. We did this for both the short- and long-cadence data, searching for a significant single peak in the power spectrum. When such a peak was detected, the most likely period was determined from a Gaussian fit to the power spectrum peak. The amplitude of variability was determined by fitting a linear combination of a sine and a constant to the light curve, at the period detected. Uncertainties in the period and the amplitude were estimated by varying these parameters until $\Delta\chi^2 = 1$ was obtained.

The detection threshold for periodicity varies from object to object, depending on its brightness, the number of quarters of observation, and possible noise characteristics specific to the object (e.g. due to backgrounds from stars at small separation). To determine these thresholds we planted, in all WDs without detected periods, sine functions with a period of 0.5 d (which is characteristic of those WDs with a detected signal), with a range of amplitudes, and found the minimum variation amplitude that is discernible in a visual examination of the power spectrum. These limits are also listed in Table 1.

To search for transient or quasiperiodic modulation, as produced by evolving spots on normal stars (see McQuillan et al. 2014), we also applied an autocorrelation-function (ACF) analysis to all of the WD time series. We did not find significant results. This, and the power-spectrum analysis results below, indicate a stable modulation.

3.2 Results

Among the 14 WDs in the sample, we detect a periodic signal in at least five, and possibly up to seven WDs. All seven detections are in the long-cadence data, with periods in the range of 2 hr to 10 days, and semi-amplitudes of 60–2100 ppm. In the short-cadence data, we rediscover the same long-timescale periodicities that we detect in the long cadence data, but we do not detect any short-timescale periodic modulations, other than several artificial periods already noted by Østensen et al. (2010, 2011). In five cases, the detection is unequivocal. In one case, KIC 11514682 the semi-amplitude (62 ppm) is low, yet we detect the same period in the data for each of three separate years (with four quarters each), lending confidence to its reality. For another WD, KIC 8682822, which has the lowest variation amplitude (60 ppm), we have only two years (eight quarters) of data. Although the same amplitude-spectrum peak frequency appears in both years, it sits on top of a broad low-frequency bump, which could be due to noise, aliasing of the real period, or real quasi-periodicity of the signal. We have further tested the reality of these two detections using a Monte-Carlo simulation. In each case, we have produced 1000 different time-scrambled versions of the light curve, and calculated the Fourier amplitude spectrum for each version. In none of the simulated cases was the amplitude of the highest peak in the spectrum, at any frequency, as high as the observed peaks. Nevertheless, we consider the detection of periodicity in KIC 11514682 as not completely conclusive, and in KIC 8682822 as only tentative.

The periods, semi-amplitudes, and their uncertainties, are listed in Table 1. Figures 1–7 show, for each of these seven WDs, a section of the processed light curve, the amplitude spectrum of the whole data set, and the period-folded light curve, binned into eight bins. For each bin we give the median of the points in that bin and draw an error bar, estimated as 1.48 times the median absolute deviation (MAD)

around the median, divided by $\sqrt{n_{bin}}$, where n_{bin} is the number of points in that bin. In all seven cases, the light curves appear sinusoidal in shape.

4 PHYSICAL MECHANISMS FOR PERIODIC PHOTOMETRIC VARIABILITY

The possible interpretations of photometric modulation are not always unique. We therefore begin by discussing, in general, the possible sources of periodic photometric variability in the range observed for these WDs.

4.1 Transits by a companion object

A companion object in a high-inclination binary orbit can produce periodic variability by means of transits. Rocky orbiting objects of sizes $\sim 50 - 200$ km could produce the observed small amplitudes. However, any transiting object would result in a characteristic dip, visible in the folded light curve during only a small fraction of an orbital period, and the power spectrum would display a series of peaks at harmonics of the orbital period. The folded light curves for the WDs with periodicities are not of this type, and thus transits can generally be ruled out. We note that, for all the other mechanisms that we discuss below, and assuming circular orbits, one expects roughly sinusoidal light curves, as observed.

4.2 Beaming due to reflex motion induced by a companion

Another potential cause of periodic variability is special-relativistic beaming of the WD light, due to orbital motion of the WD, induced by a companion. In our sample, the WDs are hot, with the *Kepler* bandpass always well on the Rayleigh-Jeans side of the thermal spectrum. The periodic signal that beaming will produce, for this case, has relative semi-amplitude $A \sim (v \sin i)/c$, where v is the orbital velocity of the WD, and i is the inclination angle between the orbital plane's axis and the line of sight (Loeb & Gaudi 2003; Zucker et al. 2007; Faigler & Mazeh 2011; Mazeh et al. 2012). For a WD mass of M_{wd} (typically $0.6 M_{\odot}$) and a companion mass M_2 , an observed period P implies a “mass function”

$$\begin{aligned} \frac{M_2 \sin i}{M_{\odot}} \left(\frac{M_2 + M_{wd}}{1.6 M_{\odot}} \right)^{-2/3} \\ = \left(\frac{A}{520 \text{ ppm}} \right) \left(\frac{P}{1 \text{ d}} \right)^{1/3}. \end{aligned} \quad (1)$$

4.3 Reflection from a companion

Alternatively to beaming, periodic modulation can be produced by WD light that is reflected from an orbiting cool companion, as it goes through illumination phases. The modulation's semi-amplitude in this case is $A \sim (D \sin i/8)(R_2/a)^2$, where D is the albedo of the companion, R_2 is its radius and a is the separation. For a $0.6 M_{\odot}$ WD and a companion of significantly lower mass, the minimum companion radius required to explain the observed

modulation (obtained when both $D = 1$ and $\sin i = 1$) is then

$$R_2 > 0.1 R_{\odot} \left(\frac{A}{100 \text{ ppm}} \right)^{1/2} \left(\frac{P}{1 \text{ d}} \right)^{2/3} \left(\frac{M_{wd}}{0.6 M_{\odot}} \right)^{1/3} \quad (2)$$

Companions with radii up to $R_2 \lesssim 0.2 R_{\odot}$ could be planets (Jupiter-mass planets up to such radii have been discovered, see e.g. Baraffe et al. 2014) or brown dwarfs. The brown-dwarf reflection option, however, is unlikely to be relevant for more than one or two of the WDs in the sample, because there is a $\lesssim 2\%$ fraction of brown-dwarf companions to WDs (Steele et al. 2011; Girven et al. 2011). A minimum companion radius above $R_2 \sim 0.2 R_{\odot}$ implies a hydrogen-burning star with $T_{\text{eff}} \gtrsim 2800$ K (e.g. Hillebrand & White 2004), which can be tested via the presence of a thermal IR signal (see below).

4.4 Thermal emission from a companion

For tight WD-companion orbits, a sub-stellar companion can be heated non-uniformly (e.g. on its tidally locked day side) by the WD. The thermal re-radiation from the heated companion hemisphere, as it goes through apparent phases, may produce observed photometric modulation. The companion's equilibrium insolation temperature will be

$$T_2 = T_{wd} \left(\frac{1-D}{f} \right)^{1/4} \left(\frac{R_{wd}}{a} \right)^{1/2}, \quad (3)$$

where f is a factor between 4 and 2, depending on whether the companion redistributes absorbed heat over its entire surface (in which case there will be no modulation from thermal re-radiation) or over only the hemisphere facing the WD (in which case it is the temperature only of that hemisphere). If heat redistribution is particularly inefficient, then a single effective temperature for the companion is poorly defined.

The flux ratio between the WD and the companion at a wavelength λ is

$$\frac{f_{WD}}{f_2} = \frac{B_{\lambda}(T_{wd})}{B_{\lambda}(T_2)} \left(\frac{R_{wd}}{R_2} \right)^2, \quad (4)$$

where $B_{\lambda}(T_{\text{eff}})$ is the thermal flux per unit wavelength at wavelength λ from an object of effective temperature T_{eff} , T_{wd} and T_2 are the effective temperatures of the WD and the companion, respectively, and R_{wd} and R_2 are their respective radii. The Wien tail from the thermal emission of an irradiated companion can enter the *Kepler* photometric bandpass, which extends from $\sim 4400 - 8800$ Å. Multiplying the numerator and denominator in the ratio in Eq. 4 by the throughput and integrating each of them over the bandpass gives twice the maximum modulation semi-amplitude (corresponding to a high line-of-sight inclination of the orbital plane) via this mechanism.

In addition, using Eq. 4, the time-independent signature of a possible stellar companion with known effective temperature of its own, whose mass is indicated, e.g., by beaming, can be tested by means of the companion's expected near-infrared or optical thermal emission, which may be comparable to that from the WD, or even dominant.

4.5 Rotation plus cold magnetic starspots

As noted, periodic photometric variations can be caused by WD rotation, combined with a spotted surface. In analogy to normal stars, stars spots in WDs may be able to form at sites where the (possibly weak) magnetic field inhibits convective motions, resulting in lower effective temperatures there. Spots are not expected in WDs whose atmospheres are fully radiative — DA WDs with $T_{\text{eff}} \gtrsim 14,000$ K, and DB WDs with $T_{\text{eff}} \gtrsim 28,000$ K. Only two of the variable WDs in our sample are cool enough for spots to explain the observed variations.

4.6 Rotation plus magnetic dichroism

Periodic photometric modulation can be caused by a heterogeneous atmospheric continuum opacity due to magnetic dichroism. As noted in Section 1.1, the amplitude depends linearly on magnetic field as $\sim B/(10^9 \text{ G})$. The observed WD semi-amplitudes listed in Table 1, of $A \sim 10^{-4}$ – 10^{-3} , would then imply surface fields of $B \sim 100$ kG to 1 MG. As we do not know the magnetic field strengths for this WD sample, each variable WD, individually, could be explained with this mechanism. However, only 5–10% of the general WD population are this highly magnetic, and therefore from a statistical point of view it is unlikely that, from our sample of 14 WDs, more than one or two would be magnetic. In any event, this possibility can be tested in the future by measuring the magnetic fields of the seven periodic WDs.

4.7 Rotation plus hot spots from magnetically channelled ISM accretion

Another rotation-based mechanism for photometric periodicity is accretion by the WD of gas from the interstellar medium (ISM, e.g. Liebert 1980), and channeling of the material onto the WD’s magnetic poles, producing hot spots that cause the observed modulation.

A WD moving through the ISM at velocity v_{ran} will have its geometric cross-section, $\sigma_g = \pi R_{\text{WD}}^2$, effectively increased through gravitational focusing to $\sigma_{\text{gf}} = \sigma_g(1 + v_{\text{esc}}^2/v_{\text{ran}}^2)$, where v_{esc} is the escape velocity from the WD surface, which is $\sim 4500 \text{ km s}^{-1}$ for a typical WD of mass $M_{\text{wd}} = 0.6 M_{\odot}$ and radius $R_{\text{WD}} \sim 8000 \text{ km}$. The minimum mass accretion rate through such direct impact of ISM gas on the WD is thus

$$\dot{M}_{\text{gf}} = \rho_{\text{ism}} \sigma_{\text{gf}} v_{\text{ran}} \quad (5)$$

$$\approx 1.6 \times 10^5 \text{ g s}^{-1} \left(\frac{n_{\text{ism}}}{1 \text{ cm}^{-3}} \right) \left(\frac{M}{0.6 M_{\odot}} \right) \left(\frac{v_{\text{ran}}}{35 \text{ km s}^{-1}} \right)^{-1},$$

where ρ_{ism} and n_{ism} are the ISM mass and volume densities, respectively, and the fiducial $v_{\text{ran}} = 35 \text{ km s}^{-1}$ is the 1σ random velocity dispersion of disk stars from Han & Gould (1995).

However, a potentially much larger accretion rate can arise in the context of Bondi-Hoyle-Lyttleton (BHL) accretion (Hoyle & Lyttleton 1941; Bondi & Hoyle 1944; see Edgar 2004 for a review), in which the gravity of the moving object focuses material from a much greater volume into

a hydrodynamical downstream conical wake, that the moving object then accretes. The BHL accretion rate is

$$\dot{M}_{\text{BHL}} = 4\pi G^2 M^2 \rho_{\text{ism}} v_{\text{ran}}^{-3} \quad (6)$$

$$= 2.7 \times 10^9 \text{ g s}^{-1} \left(\frac{M}{0.6 M_{\odot}} \right)^2 \left(\frac{n_{\text{ism}}}{1 \text{ cm}^{-3}} \right) \left(\frac{v_{\text{ran}}}{35 \text{ km s}^{-1}} \right)^{-3}.$$

The gravitational energy of this mass flow will be thermalized on impact on the surface of the WD, giving the WD an increment to its bolometric luminosity, L_{bol} , of

$$\Delta L_{\text{acc}} = \frac{1}{2} \dot{M}_{\text{BHL}} v_{\text{esc}}^2 \quad (7)$$

$$\approx 3 \times 10^{26} \text{ erg s}^{-1} \left(\frac{M}{0.6 M_{\odot}} \right)^{10/3} \left(\frac{n_{\text{ism}}}{1 \text{ cm}^{-3}} \right) \left(\frac{v_{\text{ran}}}{35 \text{ km s}^{-1}} \right)^{-3},$$

where we have assumed that R_{wd} scales roughly as $M^{-1/3}$.

Supposing the magnetic field around the WD channels this gas to the magnetic poles of the WD, and the magnetic axis is misaligned with the rotation axis, then rotating hot spots could form, that could produce photometric variability. In “polar” cataclysmic variables (CVs), an accretion disk around a WD is disrupted within a radius where the gas pressure is less than the magnetic energy density, and the mass flow is channeled to the magnetic poles (e.g. Cropper 1990). Polar CVs are seen to occur only in WDs with $B \gtrsim 10^5 \text{ G}$. However, the accretion rates in CVs are $\sim 10^7$ times higher than the BHL accretion rates considered here, so the gas density of the BHL accretion flow (which may make a transition to an accretion disk geometry at a small distance from the WD) is also likely orders of magnitude smaller than the density in the accretion disk of a CV. Channeling of the accreted material to the poles may then be possible, even with the kG-or-less magnetic fields of common WDs.

The accreted power will result in a temperature increment, ΔT , within the hot spot, which will translate to a relative increment in the optical luminosity of the WD,

$$A = \left(\frac{\Delta L}{2L} \right)_{\text{opt}} = \frac{\Delta L_{\text{acc}}}{8L_{\text{bol}}} \quad (8)$$

$$= 100 \text{ ppm} \left(\frac{\Delta L_{\text{acc}}}{10^{28} \text{ erg s}^{-1}} \right) \left(\frac{T_{\text{eff}}}{13 \text{ kK}} \right)^{-4} \left(\frac{M_{\text{wd}}}{0.6 M_{\odot}} \right)^{2/3}.$$

The incremental accretion power in the polar hot spots thus could, in principle, produce enough contrast to give the observed relative variation amplitudes of $A \sim 10^{-4}$ – 10^{-3} , if the WD mass, the ISM density, and the WD velocity result in a high enough accretion rate, and the WD temperature is not too high (which produces a high WD luminosity and hence a lower contrast of the hot spots).

Koester & Wilken (2006) considered BHL accretion from the ISM onto WDs, by way of explaining the metals observed in DAZ WD atmospheres, as resulting from ISM solar-abundance gas accretion. DAZ WDs would then be those WDs, among the full WD population, with the highest ISM accretion rates. From their calculated diffusion times of metal atoms in WD atmospheres, and the observed calcium line strengths in a sample of 38 DAZ WDs, they derived accretion rates for these WDs. Assuming the accretion is from ISM gas with a solar abundance, they obtained total

ISM mass accretion rates for DAZ WDs in the range $\dot{M} \sim 10^8 - 10^{11} \text{ g s}^{-1}$, with a median rate of $\dot{M} \sim 5 \times 10^9 \text{ g s}^{-1}$. As they knew M_{wd} and v_{ran} for every WD in their sample, they could also derive n_{ism} for each WD, under the assumption of BHL accretion. Koester & Wilken (2006) concluded that most of their DAZ WDs were passing through warm, partly-ionized, ISM clouds with $n_{\text{ism}} \sim 0.01 - 1 \text{ cm}^{-3}$.

However, by now it has become quite clear that DAZ WDs accrete their metals from circumstellar disks of rocky debris, rather than from the ISM (e.g. Farihi et al. 2010, 2012). Recalling that, in the ISM accretion picture, the 10–20% of WDs with metal lines are supposedly those WDs with the highest accretion rates, the rates found by Koester & Wilken (2006) would then constitute firm upper limits on any ISM accretion. On the other hand, if gas accreted from the ISM is channeled to the magnetic poles, it is conceivable that the ISM metal atoms would remain confined to the polar regions, before sinking locally into the WD, and hence an ISM-accreting WD might not appear as a DAZ WD after all. In such a scenario, one may expect to see an accreting WD transitioning spectroscopically, over a rotation period, between a DA and DAZ type. Indeed, WD rotation coupled with surface chemical inhomogeneity, resulting from anisotropic accretion, has been proposed as another, related mechanism to explain WD periodicity (e.g. Holberg & Howell 2011). We conclude that our proposed scenario of rotation combined with ISM accretion onto magnetic hot spots may be viable for explaining the observed periodicities and amplitudes, but, as we show below, rather extreme conditions are required in order to explain some of the observed variation amplitudes.

4.8 Rotation plus non-uniform UV line opacity and optical fluorescence

We consider one last possible mechanism to explain the periodic variability seen in our WD sample, based on rotation combined with UV opacity. As noted above, Koester et al. (2014) found, using UV spectroscopy with HST, that 56% of WDs, in the temperature range 17 kK to 27 kK (similar to the temperatures of our sample WDs), display metal absorption lines, presumably the result of recent or ongoing accretion of rocky circumstellar material. Examination of the spectra suggests that of order 1% of the UV flux is absorbed in these lines. Some fraction of the energy of the absorbed photons will be “degraded” and re-emitted as a pseudo-continuum of optical and IR photons, a process known as fluorescence. Calculations of fluorescence for the case of Type-Ia supernovae by Pinto & Eastman (2000) (in which there is extremely heavy line-blanketing by metal species) show that the fractional flux absorbed in the UV and re-emitted in the optical is comparable. If this effect operates in WD atmospheres as well, and if the accretion onto the WD is not fully uniform (e.g. due to some channeling of the flow to the poles by weak magnetic fields), a non-uniform WD optical surface brightness could result. For example, if the UV opacity, averaged over a WD hemisphere, differs by 1% between two hemispheres, and 1% of the UV flux is absorbed and fluoresces in the optical, WD rotation could then lead to the $A \sim 10^{-4}$ modulations that we see. Remarkably, the incidence of UV opacity found by Koester et al. (2014), and the incidence of WD variability

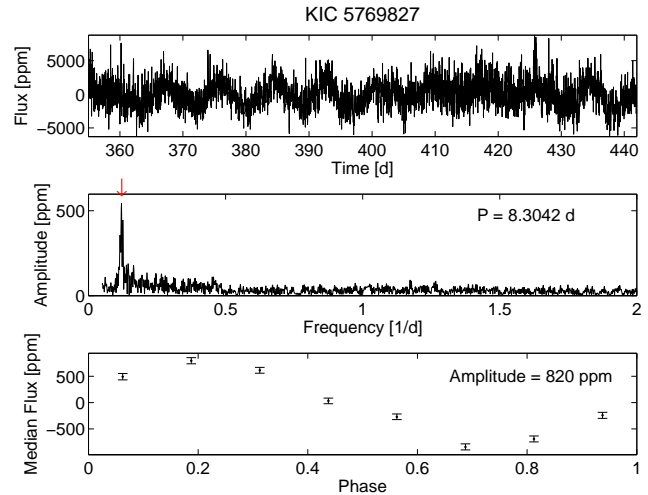


Figure 1. KIC 5769827 – Top panel: segment of the normalised light curve; middle panel: FFT amplitude spectrum; bottom panel: phase-folded and binned light curve.

that we find, are both 50%. Thus, this mechanism is one (and the only one among all of the mechanisms above) that could explain all of the cases of variability among WDs in our sample. An extreme example of a WD with non-uniform UV opacity and rotation, leading to periodic variability is the isolated WD GD 394, which is extremely metal polluted and shows EUV variations with 25 per cent amplitude and a 1.15 d period (Dupuis et al. 2000; Chayer et al. 2000). However, the viability of UV-to-optical fluorescence for the case of mildly UV-opaque WD atmospheres needs to be demonstrated by detailed calculations. Observationally, UV spectroscopy of our full WD sample could test whether there is a correspondence between the presence of UV absorption lines and optical variability.

5 INTERPRETATIONS FOR INDIVIDUAL OBJECTS

We consider now the possible physical interpretations for each of the seven WDs. Table 2 summarises how well the models fare for each WD. UV line absorption plus optical fluorescence and WD rotation, if it is a physically viable mechanism, could explain all of the variable cases, and hence we do not repeatedly state it for each individual WD below.

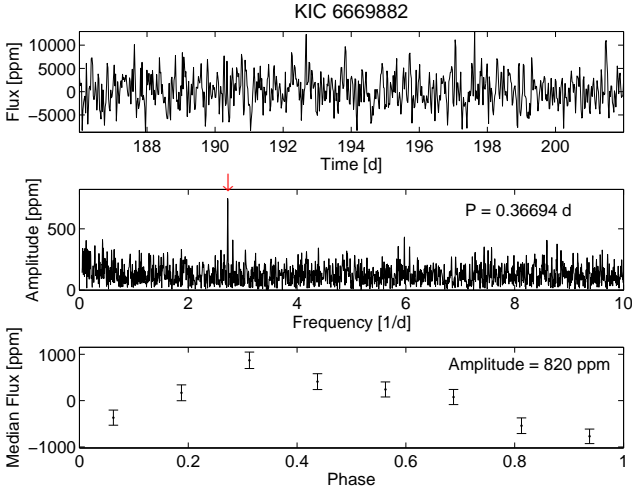
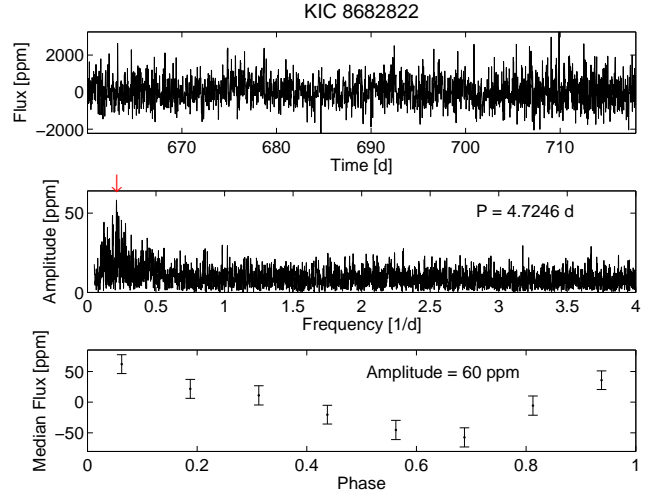
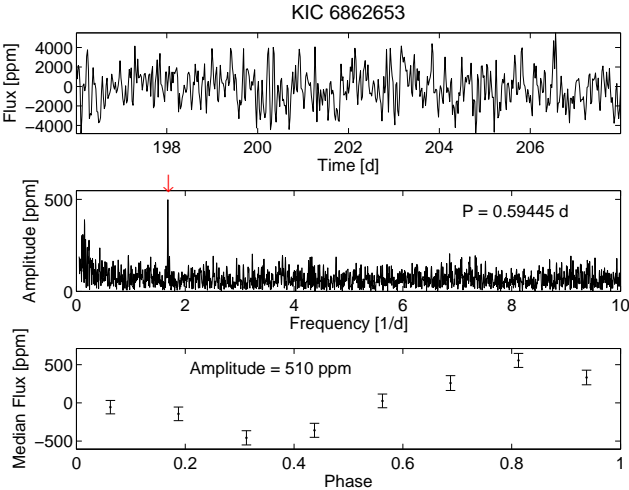
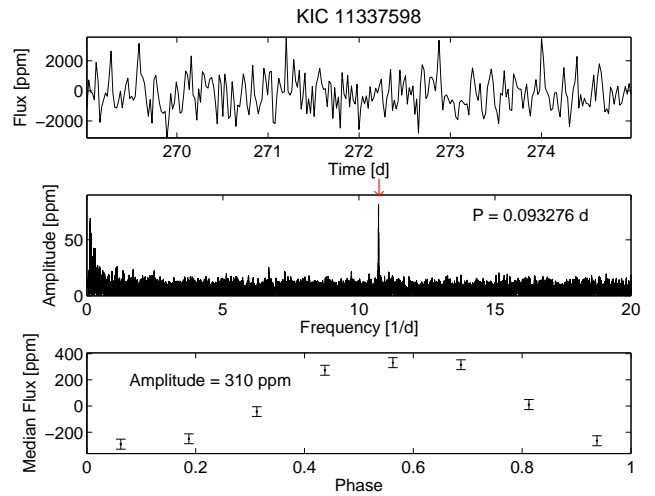
5.1 KIC 5769827 = J18547+4106

Based on the WD surface gravity, the temperature, and their uncertainties, as found by Østensen et al. (2011), this DA WD has a mass in the range $M \approx 0.6 - 1.0 M_{\odot}$. Its photometry reveals a 8.3 d period with a semi-amplitude of 820 ppm. The effective temperature is too high for cool magnetic spots. The variations can result from rotation combined with magnetic dichroism if $B \sim 1 \text{ MG}$, which is possible, but *a priori* unlikely. For the observed amplitude to be attributed to ISM accretion plus magnetic channeling, the accretion luminosity would need to be $\gtrsim 6 \times 10^{31} \text{ erg s}^{-1}$, which is extreme, but possible, if the WD mass is in the high end, the ISM density is quite high, and v_{ran} is rather low. For

Table 2. Possible interpretations

KIC	cool spot	magnetic dichroism	accretion spot	UV-optical fluorescence	beaming +WD/BD	reflection/ re-radiation
5769827	–	?	?	+	–	–
6669882	–	?	?	+	?	+
6862653	+	?	+	+	?	+
8682822	–	+	+	+	?	–
11337598	–	?	?	+	?	+
11514682	–	+	?	+	?	–
11604781	+	?	+	+	–	–

Notes: +, possible; ?, possible but statistically unlikely; –, excluded.

**Figure 2.** Same as Figure 1, for KIC 6669882.**Figure 4.** Same as Figure 1 for KIC 8682822.**Figure 3.** Same as Figure 1, for KIC 6862653.**Figure 5.** Same as Figure 1, for KIC 11337598.

beaming to explain the period and amplitude, the unseen companion must have a mass $M_2 > 15 M_\odot$, i.e. only a massive black hole could do it, and therefore it is very unlikely.

If variations are due to reflection from a companion, the companion radius would need to be at least $R_2 > 1.2R_\odot$, i.e. the radius of a G star or more massive, whose luminosity would completely dominate over the WD in the optical.

Rotation plus UV-to-optical line fluorescence, rotation plus magnetic dichroism (implying a high magnetic field), or rotation plus a high ISM accretion rate thus appear to be the only possibilities in this case.

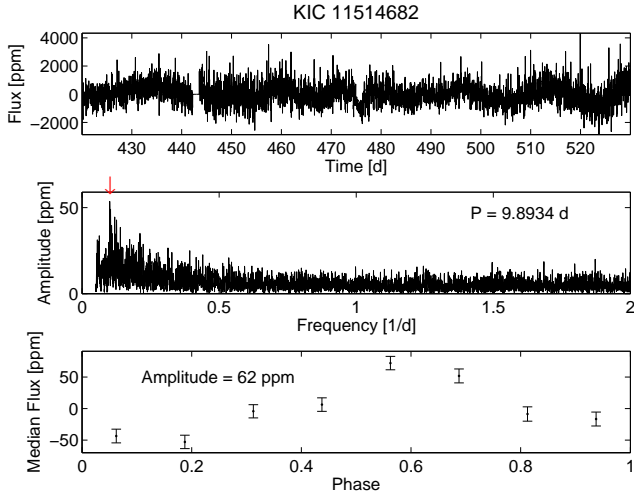


Figure 6. Same as Figure 1, for KIC 11514682.

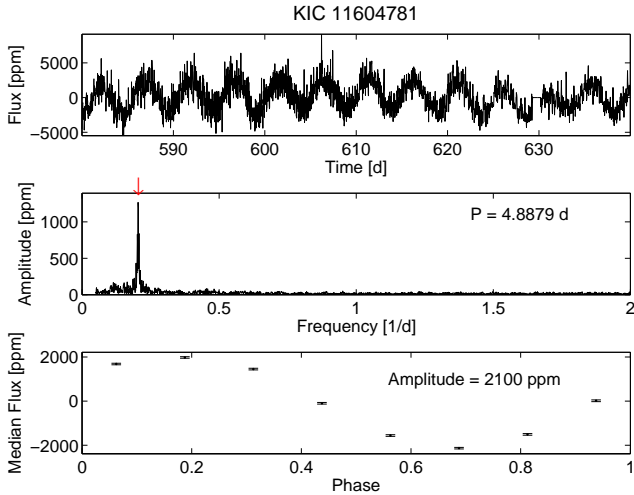


Figure 7. Same as Figure 1, for KIC 11604781.

5.2 KIC 6669882 = J18557+4207

This DA WD, which has a mass in the range $M \approx 0.40 - 0.55 M_{\odot}$ has a 820 ppm semi-amplitude modulation with a period of 8.1 hr. Østensen et al. (2011) report a 127 s periodicity in the short-cadence data, identified by us as well, which they conclude is an artifact. As in KIC 5769827, above, the WD atmosphere is too hot for the formation of convective spots. Rotation with magnetic dichroism would again require $B \sim 1$ MG. Rotation with ISM accretion onto magnetic hot spots is likewise possible, but requires a high accretion rate, $\sim 2 \times 10^{30} \text{ erg s}^{-1}$, difficult to achieve with the given low WD mass, unless v_{ran} is very small. The observed periodicity and photometric amplitude could be induced by beaming due to a $M_2 > 1 M_{\odot}$ companion. This possibility can be ruled out for a main-sequence companion, as a G-star would completely dominate over the WD in the optical spectrum. However, beaming cannot be presently ruled out if the companion is another WD (though a quite massive one, especially considering the $\sin i$ factor). In such a case, radial velocity measurements using the thermal cores of the Balmer

lines will easily detect oscillations of semi-amplitude $K \approx 200 \text{ km s}^{-1}$. However, *a priori* the probability of detecting a companion WD that induces such RV variations is $\lesssim 1\%$ (Badenes & Maoz 2012).

Alternatively, the observed modulation could also be caused by reflection off a cool companion with a minimum radius $R_2 > 0.13 R_{\odot}$, i.e. a Jupiter-like planet or a brown dwarf. The brown-dwarf option, as noted above, is *a priori* unlikely, because of the rarity of brown-dwarf companions to WDs (Steele et al. 2011; Girven et al. 2011). The insolation temperature of the companion side facing the WD, assuming it is tidally locked in this configuration, would be 1500–2300 K for a range of albedo values $D = 0.9$ to 0, making this a “hot” companion. For a Jupiter-sized planet with its day side heated to > 2000 K, the thermal re-emission by the planet, combined with the apparent orbital phases, could also give the observed amplitude of modulation, making thermal re-radiation by a substellar companion another option. Thus, the possible explanations for the observed modulation are rotation plus magnetic dichroism (though unlikely), ISM accretion (questionable), beaming due to the presence of a massive cool WD companion (also unlikely), and reflection, or re-radiation, from a giant-planet or brown-dwarf companion.

5.3 KIC 6862653 = J19267+4219

This is a $T_{\text{eff}} \sim 16,000$ K, DB-type, WD, with 14.3 hr period modulation of 510 ppm semi-amplitude. Østensen et al. (2011) could not model well its spectrum, and hence its surface gravity is unknown, and we will assume a typical WD mass of $0.6 M_{\odot}$. In DB WDs, atmospheres are convective up to $T_{\text{eff}} \gtrsim 23,000$ K, and hence cool magnetic star spots are theoretically possible in this case, and could combine with rotation to cause the observed photometric modulation. Alternatively, rotation combined with magnetic dichroism would imply a surface field of $B \sim 500$ kG, for which the probability is $\lesssim 5\%$. Rotation plus magnetic polar hotspots from ISM accretion is, again, another option, if $\Delta L_{\text{acc}} \sim 1.5 \times 10^{29} \text{ erg s}^{-1}$, which is possible for some combinations of M , n_{ism} , and v_{ran} . A $M_2 > 0.9 M_{\odot}$ companion in orbit with the WD with such a period could produce this amplitude of variability by means of beaming, but would again dominate the optical flux if it were a main-sequence star, and thus only beaming due to a cool WD companion is possible, though unlikely, because of the rarity of double WDs with such close orbits (Badenes & Maoz 2012). This possibility can be tested by the expected large $K \approx 200 \text{ km s}^{-1}$ radial velocity variations. Reflection of the WD light from a $R_2 > 0.15 R_{\odot}$ sub-stellar object could also explain the observations. It is *a priori* unlikely to be a brown-dwarf, leaving the possibility of a giant planet. Its insolation temperature would be $\sim 500 - 900$ K. In summary, in this case the most likely possibilities are cool magnetic spots, ISM-accretion-induced hot spots, and reflection from a planet.

5.4 KIC 8682822 = J19173+4452

This is a DA WD of mass $\sim 0.8 - 1.2 M_{\odot}$, in which we detect (tentatively, as explained in Section 3.2) a very small-amplitude modulation of 60 ppm, with a period of 4.7 d.

As in most of the WDs in the sample, the temperature is too high for spottedness, but rotation could work if combined with dichroism from a $B \sim 50$ kG field (which is not exceedingly rare), or with an ISM accretion rate of $\Delta L_{\text{acc}} \sim 8 \times 10^{28} \text{ erg s}^{-1}$, (which is plausible given the large WD mass). If orbital beaming is the explanation, the companion would have a mass of at least $M_2 > 0.1 M_{\odot}$, if the WD is of mass $M_{\text{wd}} > 0.8 M_{\odot}$, i.e. M_2 would be above the hydrogen-burning limit for stars. To be subdominant at $2.2\mu\text{m}$ (e.g. in the 2MASS survey), the companion would need to have a temperature $T_2 \lesssim 2000$ K, but hydrogen-burning stars have $T_{\text{eff}} \gtrsim 2800$ K. However, another WD that is cool and of very low mass, or cool and in a low-inclination (nearly face-on) orbit could induce beaming at a level consistent with the observed variations. The expected RV semi-amplitude of the visible WD would be $K = 15 \text{ km s}^{-1}$, which is challenging but observable. If the source of photometric variability is, instead, reflection off a cool companion, it implies a minimum companion radius $R_2 \gtrsim 0.2 R_{\odot}$, or even larger if the albedo is not unrealistically close to $D = 1$, and the inclination is not close to 90° ; this required radius is at the limit of known substellar objects (e.g. Baraffe et al. 2014), and hence the thermal emission from such a hydrogen-burning companion would again have been detected. Thus, the possible (though not equally plausible) options are WD rotation plus dichroism or ISM accretion, or beaming due to a cool WD companion that is either of low mass or in a near-face-on orbit.

5.5 KIC 11337598 = J18577+4909

This $\sim 0.8 - 1.2 M_{\odot}$ DA WD has the shortest periodicity that we find, $P = 2.24$ hr, with a semi-amplitude of 310 ppm, already noted by Østensen et al. (2011) and identified by them as a possible rotation signature. T_{eff} is again too high for spots. Rotation combined with magnetic dichroism from a $B \sim 350$ kG field, or ISM accretion onto magnetic-pole hot spots with $\Delta L_{\text{acc}} \sim 6 \times 10^{29} \text{ erg s}^{-1}$, could be the explanation. If the WD mass is indeed high, such an accretion rate may be achievable. If beaming due to a companion were to produce the modulation, it would imply a minimum companion mass of $M_2 > 0.25 M_{\odot}$. To avoid being dominant at $2.2\mu\text{m}$, a main-sequence companion would need to have a temperature $T_{\text{eff},2} \lesssim 2000$ K, considerably less than the $T_{\text{eff}} \gtrsim 3200$ K of hydrogen-burning stars above such mass. The companion could, however, be a cool WD. Alternatively, reflection of the WD light by a planet with $R_2 > 0.04 R_{\odot}$ (a “Neptune”), or by a brown dwarf, could give the variation amplitude. The insolation temperature is 1200–2300 K, i.e. this would be another hot planet. If the albedo is low (giving a temperature close to 2300 K) and the planet radius is somewhat larger, thermal re-radiation can also produce the observed modulation. For higher albedos, reflection and thermal re-radiation can contribute comparably, or reflection will dominate. Interestingly, Østensen et al. (2011), when modeling the spectrum of this WD, noted its extremely broad line cores. If broadened by rotation, they imply rotation with $v \sin i = 1500 \text{ km s}^{-1}$, about half the break-up speed, which would mean a period of ~ 40 s, yet only the 2.24 hr period appears in the power spectrum. Østensen et al. (2011) proposed, alternatively, unresolved Zeeman splitting as a possible explanation of the broad line

cores. In summary, in this WD the modulation can be explained by rotation with dichroism (somewhat unlikely, but would explain also the line profiles), rotation plus ISM accretion, beaming due to a WD companion, and reflection or thermal re-radiation from a brown dwarf or a hot planet.

5.6 KIC 11514682 = J19412+4925

This DA WD has a mass in the range $M \approx 0.45 - 0.6 M_{\odot}$. We detect in its light curve a small but significant, $A = 62$ ppm semi-amplitude, modulation with a period of 9.9 d. It is too hot for spots, but rotation combined with an uneven surface brightness due to magnetic dichroism (with $B \sim 35$ kG) or to ISM accretion and magnetic channeling (with $\Delta L_{\text{acc}} \sim 2 \times 10^{29} \text{ erg s}^{-1}$) are viable explanations. For the ISM accretion to work, n_{ism} would need to be large and v_{ran} small, given that the WD mass is on the low side. Beaming induced by a companion brown dwarf with mass at the hydrogen-burning limit, $M_2 \approx 0.07 M_{\odot}$, is possible but *a priori* unlikely because of the rarity of such brown-dwarf companions. For reflection from a sub-solar companion, the companion radius would need to be $R_2 > 0.25 R_{\odot}$, which is larger than any known planet. For an albedo $D = 0.8$, a companion’s insolation temperature would be only 500 K, making thermal re-radiation also a non-option. Thus, in this case, rotation, or beaming due a sub-stellar companion, are the possible alternatives.

5.7 KIC 11604781 = J19141+4136

In this $\approx 0.6 - 1.0 M_{\odot}$ WD we detect a 4.88 d periodicity with a semi-amplitude of 0.2 per cent. This is the largest amplitude we find, and it approaches the smallest periodic variation amplitudes ($\gtrsim 0.3$ per cent) detected in ground-based observations of the magnetic WD sample of Brinkworth et al. (2013). This is also the coolest ($T_{\text{eff}} = 9,100$ K) WD in the sample (it was selected solely based on reduced proper motion, rather than UV excess). The same periodicity that we detect was found and noted by Østensen et al. (2011). The periodicity could arise through rotation combined with cool magnetic spots, dichroism (a rare $B \sim 2$ MG field would be required), or ISM accretion (a moderate accretion rate, $\Delta L_{\text{acc}} \sim 6 \times 10^{28} \text{ erg s}^{-1}$, is sufficient due to the relatively low luminosity of the WD). The variation amplitude, if caused via beaming, would require orbital motion with $v \sin i = 600 \text{ km s}^{-1}$, implying an unseen $M > 120 M_{\odot}$ black hole companion, which is unrealistic. Reflection by a companion would require a companion radius $R_2 > 1.3 R_{\odot}$, i.e. a sun-like star that would overwhelm the WD spectrum in the optical. In this case, WD rotation appears to be the only option to explain the photometric variations, through cool convection-inhibiting spots, hot ISM-accretion spots, (less likely) magnetic dichroism in a strong field, or (as viable also for all of the variable WDs) UV line absorption plus optical fluorescence.

6 DISCUSSION

We have analyzed a small sample of 14 WDs observed by *Kepler* and studied by Østensen et al. (2010, 2011). The sample selection methods suggest that most, if not all, are normal

WDs, rather than WDs with strong surface magnetic fields. We have detected 2 hr to 10-day timescale photometric variability in seven of the WDs, at amplitude levels lower than those that could be seen previously in WDs. In five of the seven cases the periodicity is unambiguous, in one case it is highly significant, and in one it is tentative. The variability could arise from WD rotation combined with non-uniform surface emission, be it due to cool magnetic spots, hot spots from ISM material channeled to magnetic poles, magnetic dichroism, or perhaps non-uniform UV line opacity and optical fluorescence. In five cases, the WDs are too hot for convection-inhibited cool magnetic spots, and in five cases the high magnetic fields required by magnetic dichroism are rather unlikely to be present. The ISM accretion rates required to reproduce the observed amplitudes are quite high, but not impossible. The fluorescence option looks promising, especially in view of the similar incidence, of UV line absorption in WDs on the one hand, and of variability in our sample, on the other hand. Accurate measurements of the WD masses, magnetic fields, random velocities, ISM densities along the line of sight, and UV spectra, could permit a clearer test of the rotation option.

In five of the cases, we cannot rule out the possibility that the variability results from beaming due to orbital motion caused by cool, low-mass, companion WDs, or by reflection from cool orbiting giant planets or brown dwarfs. In two of those five cases thermal re-radiation by the substellar companion is also possible. The WD-companion-beaming option can be tested via followup observations in search of the large radial-velocity variations expected in the primary WD spectrum. The WD companion possibility is unlikely, certainly for more than one or two of the WDs, given the observed statistical rarity of close WD pairs. Similarly, it is unlikely that more than one or two of 14 WDs would have brown-dwarf companions – such a fraction is far above the $\lesssim 2\%$ fraction from direct near-IR searches for brown dwarfs (Girven et al. 2011). However, planets of sub-Jupiter to Jupiter size, if they are abundant at these orbits around WDs, could explain three or four cases.

Figure 8 shows the seven periods and amplitudes we have measured, along with the ground-based measurements by Brinkworth et al. (2004, 2005, 2013), for 10 magnetic WDs with fairly precise rotation periods (out of 23 WDs monitored by them, 14 of them with sensitivity to periods of up to a week). Also plotted is a point for the $T = 34,000$ K DA WD BOKS53856, for which Holberg & Howell (2011) have measured, using *Kepler*, amplitude $A = 2.5\%$ variations with a period $P = 0.255$ day. In the rotation models, one does not obviously expect a relation between period (which reflects rotation rate) and photometric amplitude (which indicates the degree of surface heterogeneity), unless the magnetic field strength correlates with period. In the beaming scenario and in the planet/brown-dwarf reflection/re-radiation scenario, longer periods, corresponding to larger separations, would anti-correlate with amplitude. We include in Figure 8 several curves showing the maximal variation amplitudes as a function of period for these scenarios, for some combinations of parameters. A $0.6 M_{\odot}$ WD and $\sin i = 1$ is assumed in every curve. The line for the beaming model assumes a $M_2 = 1 M_{\odot}$ companion (e.g. an unseen cool WD of this mass). The lines for reflection by a substellar companion are for the maximal albedo,

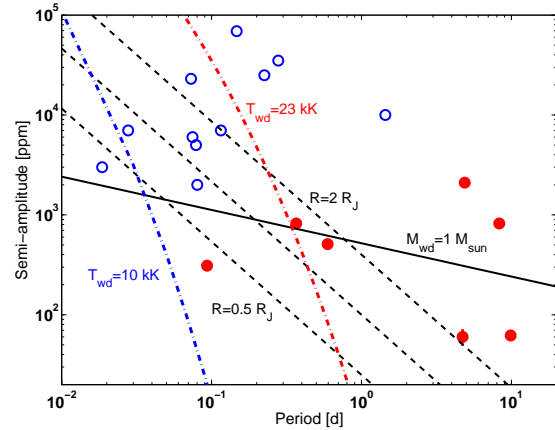


Figure 8. Variation amplitude vs. period for white dwarfs with measured periods. Red filled circles are from this study, blue empty circles are from the sample of magnetic WDs studied by Brinkworth et al. (2004, 2005, 2013) plus the WD from Holberg & Howell (2011). Curves are the maximum possible amplitudes in several models. Solid black line: beaming due to reflex motion induced by a $1 M_{\odot}$ (e.g. a WD) companion. Dashed black lines: reflection by a substellar companion with 0.5, 1.0, and 2 Jupiter radius. Dash-dot curves: thermal re-radiation from a 2-Jupiter-radius substellar companion, for two WD temperatures, one (red) characteristic of our sample, and one (blue) of the Brinkworth et al. sample’s temperatures. All models assume an $M_{\text{wd}} = 0.6 M_{\odot}$ WD and $\sin i = 1$.

$D = 1$, and for three possible companion radii, as marked. The thermal re-radiation curves are calculated for the *Kepler* bandpass, assuming the maximal $R = 0.2 R_{\odot}$ companion radius, for two WD effective temperatures, $T_{\text{wd}} = 10$ kK characteristic of the Brinkworth et al. (2013) sample, and $T_{\text{wd}} = 23$ kK typical of our sample.

The figure illustrates, for each WD, what are the allowed mechanisms from among these options (as discussed in more detail for each case in Section 5). Interestingly, the Brinkworth et al. WDs, which have larger amplitudes than our sample (only such large amplitudes were detectable by their ground-based data), have shorter periods, typically in the sub-day range. Rather than spottedness (the favoured explanation by Brinkworth et al.), we see that reflection or re-radiation from planets could be the cause for some of those WDs below the maximum-amplitude vs. period relations, plotted in Figure 8. It is also remarkable that Brinkworth et al. found clear periodic variations in 10 out of 23 WDs they studied, again a $\sim 50\%$ fraction. If fluorescence is the cause in that sample as well, the larger variation amplitudes could result from the stronger magnetic fields of their sample’s WDs, which could lead to stronger channeling of the accretion flow, and hence to a more non-uniform UV opacity and optical re-emission.

Some cases appear to defy most of the proposed explanations. Brinkworth et al. (2013) have detected, in the WD PG1658+441, rather large-amplitude (2%) variability, with a probable period between 6 hr and 4 d (not included in Figure 8 because of its uncertain period). This is a DA-type WD with $T_{\text{eff}} = 30,500$ K, i.e. too hot for spots, and with $B = 3.5$ MG, a field an order of magnitude too low for magnetic dichroism-induced variability of this am-

plitude. Furthermore, infrared observations have excluded also the presence of companions above 10 Jupiter masses (Hansen et al. 2006; Farihi et al. 2008). Very similarly, the WD BOKS53856 ($T = 34,000$ K, $P = 0.255$ day, $A = 2.5\%$, plotted) likely has only $B \sim 350$ kG. Holberg & Howell (2011) have proposed, as an explanation, rotation combined with chemical abundance-induced temperature variations over the stellar surface, likely associated with ongoing accretion (not dissimilar to our proposed mechanism of fluorescence).

If some of the seven cases of periodic variations in our sample result from WD rotation (with the modulation due to spots, dichroism, or accretion), then our results are among the few accurate measurements of rotation periods in common (DA and DB) WDs that are non-pulsating and not necessarily magnetic. This is made possible by the photometric precision of *Kepler*, which permits detecting variations at much subtler levels than previously possible. While we have measured periods for only five to seven WDs, the periods are all relatively long, and of the same order as the rotation periods previously found for more peculiar WDs. This may hint that slow WD rotation is the norm, and fast-rotating WDs may indeed be rare among the full WD population.

Alternatively, if the correct interpretation of our results is that of reflection or re-radiation from planets, then hot giant planets are extremely common around WDs, even if this interpretation is true for only a few of the seven dwarfs. Indeed, considering that the detection limits for several of the WDs without detected variability are above some of the detected amplitudes, a majority of WDs could have such planets. Such a discovery, while dramatic, would not be completely unexpected, given the recent accumulating evidence for the presence, around many WDs, of dust-and-gas disks, and ongoing accretion of rocky debris (see Section 1.2). If snowline-region Neptunes exist around many stars, as indicated by microlensing planet surveys (Gould et al. 2010; Cassan et al. 2012; Shvartzvald et al. 2014) and inward migration of such planets is frequent in the protoplanetary phase (e.g. Trilling et al. 1998; Ida & Lin 2008), it is conceivable that post-stellar migration of surviving outer planets could frequently occur around WDs. In this process, the observed disks around WDs might play a similar role to that of proto-planetary disks around young stars.

To summarise, we have reported the first detections of periodic modulations in WDs at amplitudes $\lesssim 10^{-3}$. More work is required to understand this uncharted territory. Our results highlight the need and the possibility, already being pursued, of obtaining such measurements for larger samples of WDs as part of the K2 *Kepler* Mission extension. Even larger WD samples with time-domain information will come from the *Gaia*, TESS, and PLATO missions. With such samples, it will be possible to search for relations between periodic variations and other intrinsic properties of WDs. This should help discriminate among the diverse explanations for the intriguing periodic variability, seen in the small sample studied here.

ACKNOWLEDGMENTS

We thank J. Farihi, B. Gaensicke, T. Marsh, E. Nakar, and the anonymous referee for useful advice and input. E. Gold-

stein is thanked for his significant contributions to the later versions of the paper. D.M and T.M acknowledge support from the Planning and Budgeting Committee's Israeli Centers of Research Excellence (I-CORE, grant No. 1829/12). T.M. acknowledges support from the European Research Council under the EU's Seventh Framework Programme (FP7/(2007-2013)/ERC Grant Agreement No. 291352), and by the Israel Science Foundation (grant No. 1423/11). This research has made use of the NASA Exoplanet Archive, which is operated by the California Institute of Technology, under contract with the National Aeronautics and Space Administration under the Exoplanet Exploration Program. All of the data presented in this paper were obtained from the Mikulski Archive for Space Telescopes (MAST). STScI is operated by the Association of Universities for Research in Astronomy, Inc., under NASA contract NAS5-26555. Support for MAST for non-HST data is provided by the NASA Office of Space Science via grant NNX09AF08G and by other grants and contracts.

REFERENCES

- Agol, E. 2011, *ApJ*, 731, L31
- Amaro-Seoane, P., Aoudia, S., Babak, S., et al. 2013, *GW Notes*, Vol. 6, p. 4-110, 6, 4
- Angel, J. R. P., Borra, E. F., & Landstreet, J. D. 1981, *ApJS*, 45, 457
- Badenes, C., & Maoz, D. 2012, *ApJ*, 749, L11
- Baraffe, I., Chabrier, G., Fortney, J., & Sotin, C. 2014, *arXiv:1401.4738*
- Batalha, N. M., Rowe, J. F., Bryson, S. T., et al. 2013, *ApJS*, 204, 24
- Berger, L., Koester, D., Napiwotzki, R., Reid, I. N., & Zuckerman, B. 2005, *A&A*, 444, 565
- Bondi, H., & Hoyle, F. 1944, *MNRAS*, 104, 273
- Brinkworth, C. S., Burleigh, M. R., Wynn, G. A., & Marsh, T. R. 2004, *MNRAS*, 348, L33
- Brinkworth, C. S., Marsh, T. R., Morales-Rueda, L., et al. 2005, *MNRAS*, 357, 333
- Brinkworth, C. S., Burleigh, M. R., Lawrie, K., Marsh, T. R., & Knigge, C. 2013, *ApJ*, 773, 47
- Cantiello, M., Mankovich, C., Bildsten, L., Christensen-Dalsgaard, J., & Paxton, B. 2014, *ApJ*, 788, 93
- Cassan, A., Kubas, D., Beaulieu, J.-P., et al. 2012, *Nature*, 481, 167
- Charpinet, S., Fontaine, G., Brassard, P., et al. 2011, *Nature*, 480, 496
- Chayer, P., Kruk, J. W., Ake, T. B., et al. 2000, *ApJ*, 538, L91
- Cropper, M. 1990, *Space Sci. Rev.*, 54, 195
- Debes, J. H., Hoard, D. W., Wachter, S., Leisawitz, D. T., & Cohen, M. 2011, *ApJS*, 197, 38
- Debes, J. H., Walsh, K. J., & Stark, C. 2012, *ApJ*, 747, 148
- Di Stefano, R., Voss, R., & Claeys, J. S. W. 2011, *ApJ*, 738, L1
- Dupuis, J., Chayer, P., Vennes, S., Christian, D. J., & Kruk, J. W. 2000, *ApJ*, 537, 977
- Edgar, R. 2004, *New Astronomy Reviews*, 48, 843
- Faigler, S., & Mazeh, T. 2011, *MNRAS*, 415, 3
- Faigler, S., Mazeh, T., Quinn, S. N., Latham, D. W., & Tal-Or, L. 2012, *ApJ*, 746, 185

- Farihi, J., Becklin, E. E., & Zuckerman, B. 2008, *ApJ*, 681, 1470
- Farihi, J., Barstow, M. A., Redfield, S., Dufour, P., & Hambly, N. C. 2010, *MNRAS*, 404, 2123
- Farihi, J., Gänsicke, B. T., Wyatt, M. C., et al. 2012, *MNRAS*, 424, 464
- Farihi, J., Gänsicke, B. T., & Koester, D. 2013, *Science*, 342, 218
- Ferrario, L., Vennes, S., Wickramasinghe, D. T., Bailey, J. A., & Christian, D. J. 1997, *MNRAS*, 292, 205
- Fontaine, G., Brassard, P., & Charpinet, S. 2013, *European Physical Journal Web of Conferences*, 43, 5011
- Gänsicke, B. T., Koester, D., Farihi, J., et al. 2012, *MNRAS*, 424, 333
- Girven, J., Gänsicke, B. T., Steeghs, D., & Koester, D. 2011, *MNRAS*, 417, 1210
- Gould, A., Dong, S., Gaudi, B. S., et al. 2010, *ApJ*, 720, 1073
- Greiss, S., Gänsicke, B. T., Hermes, J. J., et al. 2014, *MNRAS*, 438, 3086
- Han, C., & Gould, A. 1995, *ApJ*, 447, 53
- Hansen, B. M. S., Kulkarni, S., & Wiktorowicz, S. 2006, *AJ*, 131, 1106
- Hoard, D. W., Debes, J. H., Wachter, S., Leisawitz, D. T., & Cohen, M. 2013, *ApJ*, 770, 21
- Holberg, J. B., Sion, E. M., Oswalt, T., et al. 2008, *AJ*, 135, 1225
- Holberg, J. B., & Howell, S. B. 2011, *AJ*, 142, 62
- Howell, D. A., Sullivan, M., Nugent, P. E., et al. 2006, *Nature*, 443, 308
- Hoyle, F., & Lyttleton, R. A. 1941, *MNRAS*, 101, 227
- Ida, S., & Lin, D. N. C. 2008, *ApJ*, 673, 487
- Ilkov, M., & Soker, N. 2012, *MNRAS*, 419, 1695
- Justham, S. 2011, *ApJ*, 730, L34
- Kamiya, Y., Tanaka, M., Nomoto, K., et al. 2012, *ApJ*, 756, 191
- Karl, C. A., Napiwotzki, R., Heber, U., et al. 2005, *A&A*, 434, 637
- Kawaler, S. D. 2004, *Stellar Rotation*, 215, 561
- Kawka, A., Vennes, S., Schmidt, G. D., Wickramasinghe, D. T., & Koch, R. 2007, *ApJ*, 654, 499
- Kepler, S. O., Pelisoli, I., Jordan, S., et al. 2013, *MNRAS*, 429, 2934
- Kilic, M., Brown, W. R., & McLeod, B. 2010, *ApJ*, 708, 411
- Koester, D., & Wilken, D. 2006, *A&A*, 453, 1051
- Koester, D., Gänsicke, B. T., & Farihi, J. 2014, *A&A*, 566, 34
- Liebert, J. 1980, *ARA&A*, 18, 363
- Loeb, A., & Gaudi, B. S. 2003, *ApJ*, 588, L117 99
- Loeb, A., & Maoz, D. 2013, *MNRAS*, 432, L11
- Maoz, D., Mannucci, F., & Nelemans, G. 2013, *ARA&A*, 52, 107
- Martin, D. C., Fanson, J., Schiminovich, D., et al. 2005, *ApJ*, 619, L1
- Maxted, P. F. L., & Marsh, T. R. 1999, *MNRAS*, 307, 122
- Mazeh, T., Naef, D., Torres, G., et al. 2000, *ApJ*, 532, L55
- Mazeh, T., Nachmani, G., Sokol, G., Faigler, S., & Zucker, S. 2012, *A&A*, 541, A56
- McQuillan, A., Mazeh, T., & Aigrain, S. 2014, *ApJS*, 211, 24
- Mosser, B., Goupil, M. J., Belkacem, K., et al. 2012, *A&A*, 548, A10
- Nordhaus, J., & Spiegel, D. S. 2013, *MNRAS*, 432, 500
- Østensen, R. H., Silvotti, R., Charpinet, S., et al. 2010, *MNRAS*, 409, 1470
- Østensen, R. H., Silvotti, R., Charpinet, S., et al. 2011, *MNRAS*, 414, 2860
- Pinto, P. A., & Eastman, R. G. 2000, *ApJ*, 530, 757
- Shvartzvald, Y., Maoz, D., Kaspi, S., et al. 2014, *MNRAS*, 439, 604
- Silverman, J. M., Ganeshalingam, M., Li, W., et al. 2011, *MNRAS*, 410, 585
- Slawson, R. W., Prša, A., Welsh, W. F., et al. 2011, *AJ*, 142, 160
- Soker, N. 2013, *New Astronomy*, 18, 18
- Steele, P. R., Burleigh, M. R., Dobbie, P. D., et al. 2011, *MNRAS*, 416, 2768
- Tout, C. A., Wickramasinghe, D. T., Liebert, J., Ferrario, L., & Pringle, J. E. 2008, *MNRAS*, 387, 897
- Trilling, D. E., Benz, W., Guillot, T., et al. 1998, *ApJ*, 500, 428
- Villaver, E., & Livio, M. 2009, *ApJ*, 705, L81
- Winget, D. E., & Kepler, S. O. 2008, *ARA&A*, 46, 157
- Wood, M. A. 1995, *White Dwarfs*, 443, 41
- Yanny, B., Rockosi, C., Newberg, H. J., et al. 2009, *AJ*, 137, 4377
- Yoon, S.-C., & Langer, N. 2004, *A&A*, 419, 623
- Zucker, S., Mazeh, T., & Alexander, T. 2007, *ApJ*, 670, 1326